

# Analyst

Accepted Manuscript



This is an *Accepted Manuscript*, which has been through the Royal Society of Chemistry peer review process and has been accepted for publication.

*Accepted Manuscripts* are published online shortly after acceptance, before technical editing, formatting and proof reading. Using this free service, authors can make their results available to the community, in citable form, before we publish the edited article. We will replace this *Accepted Manuscript* with the edited and formatted *Advance Article* as soon as it is available.

You can find more information about *Accepted Manuscripts* in the [Information for Authors](#).

Please note that technical editing may introduce minor changes to the text and/or graphics, which may alter content. The journal's standard [Terms & Conditions](#) and the [Ethical guidelines](#) still apply. In no event shall the Royal Society of Chemistry be held responsible for any errors or omissions in this *Accepted Manuscript* or any consequences arising from the use of any information it contains.

1  
2  
3 **Response to the referees' comments and suggestions on the paper titled "Effect of**  
4 **Hematocrit on Blood Dynamics on a Compact Disc Platform" (Manuscript ID**  
5 **AN-COM-11-2014-002020)**  
6

7  
8 Authors would like to thank the referees for the appreciation of the reported study, and the  
9 constructive suggestions for further improvement of the reported work. The details of the  
10 responses against the specific questions/queries raised by the reviewers are illustrated below.  
11

12 **Response to comments of Referee -1 (suggested minor revisions)**  
13

14 **#1 Referee's comment:** *p3, line 36-38: "The valving... is governed by the balance of*  
15 *centrifugal forces and the capillary forces." It is true, but might be just part of forces*  
16 *involved. For example, is the height of liquid in the inlet reservoir playing a part as a result of*  
17 *gravity force? Also, what is the direct of the capillary force in this system which is hinted in*  
18 *the above mentioned sentence to be opposite to centrifugal force? Therefore, more*  
19 *discussion/clarifications needed about it.*  
20  
21

22 **#1 Authors' response:** Authors would like to thank the referee for pointing out the above  
23 issue. The effect of gravity force will also work on the liquid of the inlet reservoir. From  
24 order of magnitude analysis, we found that the ratio of the capillary force acting on the liquid  
25 column of inlet reservoir to the weight of the liquid in the inlet reservoir is  $\sim O(10^4)$ . For that  
26 reason, the gravity effect was not considered during our investigation.  
27

28 Below a threshold frequency, the fluid will not come out from the inlet reservoir, as the  
29 capillary force overshadows the centrifugal force (these forces tend to oppose each other, for  
30 the regimes of contact angle addressed in this work). Beyond the threshold frequency,  
31 however, the centrifugal force overcomes the surface tension force, and the fluid starts  
32 flowing in the radial direction (as shown in Fig. 1b in the revised manuscript). This has been  
33 elucidated in our revised manuscript.  
34

35 **#2 Referee's comment:** *p4 Fig 4b: The disagreement between theoretical and experimental*  
36 *results at higher speeds needs more analysis. Similar to above point, there might be other*  
37 *important factors playing a part, such as flow resistance along the channel which varies*  
38 *under different conditions during rotation.*  
39

40 **#2 Authors' response:** Authors would like thank the reviewer for highlighting the above  
41 point. Possibly, at higher speed of rotation, mechanical vibration of the experimental set-up  
42 plays a key role, which results in the observed deviation between experimental and  
43 simulation results. This issue has been clarified in the revised manuscript. Accordingly, we  
44 have inferred from our studies that 200 rpm may be the maximum speed limit upto which we  
45 may safely use our predictive design tool based on theoretical simulations.  
46  
47

48 **#3 Referee's comment:** *Careful proof-reading is needed as a number of language errors or*  
49 *typos scatter throughout the text. e.g. p2 line42 "it were stored...", sentence in p2 line50-51,*  
50 *p2 equations having square signs, etc.*  
51

52 **#3 Authors' response:** The aforementioned issues have been well-addressed in the revised  
53 manuscript.  
54  
55  
56  
57  
58  
59  
60

## Response to comments of Referee -2

### **Rationale:**

**#1 Referee's comment:** *Authors try to justify their case by stating that blood rheology is altered in diseases like malaria and sickle cell anemia. While I don't argue against this statement, I am not also convinced that blood rheology is simply affected by the hematocrit level, as the subsequent experiments try to impress. The reliability of hematological parameters such hematocrit level in predicting malarial infection remains questionable (Muwonge et al., ISRN Tropical Medicine, 2013). Also a survey of hematocrit level among malaria-infected patients show a big spread in hematocrit level (20-60%; Lee et al. Malaria Journal 2008 7:149). Hence, authors should present their case and the rationale behind the study with more objective argument. I did not find any mention of hematocrit-disease relation in Refs. 1 and 3.*

**#1 Authors' response:** It has been illustrated in literature (J. D. Enderle et al, *Introduction to Biomedical Engineering, Academic Press, San Diego, Third., 2005*, D. J. Schneck et al, *Biofluid Mechanics, University Press, New York, New York, 1990*) that the rheological nature of blood is dependent on several parameters like number of cells suspended, size and shape of the suspended cells, extent of cellular interactions, mechanical properties of cells, and chemistry of plasma solutions. From literature (M. Diez-Silva et al, *MRS Bull.*, **35**, 382–388, O. K. Baskurt et al, *Semin. Thromb. Hemost.*, 2003, **29**, 435–450, F. K. Glenister et al, *Blood*, 2002, **99**, 1060–1063), it is also evident that the morphological alterations of RBCs (which is pertinent in case of few diseases like malaria, sickle cell anemia) have significant impact over blood rheology. It has further been emphasized in the literature (J. D. Enderle et al, *Introduction to Biomedical Engineering, Academic Press, San Diego, Third., 2005*) that effective viscosity of a blood sample may depend on (a) ~~the~~ chemistry of the plasma, specifically its globular protein composition, (b) the chemistry of the red blood cell, specifically its hemoglobin concentration, (c) the number (hematocrit), size (MCV, RBC diameter, and surface area), and degree of cellular aggregation (rouleaux) of red blood corpuscles, (d) the erythrocyte shape, geometry (degree of cell biconcavity), and deformability; and, (e) the mass density of RBCs, plasma, and the composite whole blood. Based on these considerations, functional correlations between the effective viscosity of a blood sample and its hematocrit level have been well documented in the literature, over a typical range of hematocrit levels of 0 to 50 (for example, see: Y. C. Fung, *Biomechanics. Mechanical properties of living tissues, Springer, Berlin, 1993*; E. W. Merrill, *Physiological Reviews*, 1969, **5**, 863-888). In our simulations, we have used one such commonly invoked correlation for modeling blood rheology, which corroborates widely with experimental data. This rheological alteration, in turn, alters the observed flow dynamics on a rotational platform, which we consider as the fundamental rationale behind our predictive strategy.

### **Results:**

**#1 Referee's comment:** *Why did the authors chose to vary  $W$  instead of  $H$ ? If the microhydrodynamic principles are to be respected, then at  $H/W < 1$ , hydrodynamics should*

1  
2  
3 *be governed more by H and in reality blood vessels are more circular than rectangular. What*  
4 *is justification for the observed variation of fb with W in Figure 3? These issues should be*  
5 *clarified. Also, please avoid using confusing terms such as “different dimensions of the*  
6 *channel”. Simply mention width or W.*

7  
8 **#1 Authors' response:** Authors would like to express sincere thanks to the referee for  
9 pointing out the issue. This confusion has primarily arisen because of a possible confusion of  
10 different terminologies adopted in the literature concerning height and width. Here, we have  
11 termed the smaller of the two dimensions as the width, which in turn dictates the hydraulic  
12 diameter, and hence governs the physics of micro-hydrodynamics.

13  
14  
15 During the flow of blood through micro-conduits, there is a formation of cell-free-layer  
16 (CFL) at the vicinity of channel walls (*R. Fahraeus et al, Am. J. Physiol., 1931, 96, 562–568,*  
17 *J. H. Barbee et al, Microvasc. Res., 1971, 3, 17–21*). The extent of CFL zone varies with the  
18 varying hydraulic diameter of the channel as reported by *A R. Pries et al. (Am. J. Physiol.,*  
19 *1992, 263, 1770–1778)*. For that reason, the authors have investigated the effect of different  
20 hydraulic diameters in the present study. The concerned issue has been addressed in the  
21 revised version of the manuscript, in a manner as detailed below.

22  
23  
24  
25 We have emphasized in our revised manuscript that the concentration of RBCs is more at the  
26 central zone of the channel as compared to the vicinity of the channel-wall (*J. D. Enderle et*  
27 *al, Introduction to Biomedical Engineering, Academic Press, San Diego, Third., 2005*). This  
28 heterogeneity of cell distribution is the manifestation of the net hydrodynamic force. For a  
29 particular Hct, higher the channel hydraulic diameter, lower is the extent of cell free layer  
30 (CFL). Hence the effective viscosity becomes lower for the higher hydraulic diameter, which  
31 makes the volumetric flow rate higher. The heterogeneous distribution of cells is known to be  
32 altered with the channel hydraulic diameter (*A R. Pries, D. Neuhaus, and P. Gaehtgens, Am.*  
33 *J. Physiol., 1992, 263, 1770–1778; A. Kazemzadeh, P. Ganesan, F. Ibrahim, S. He, and M. J.*  
34 *Madou, PLoS One, 2013, 8, e73002.; R. Fahraeus and T. Lindqvist, Am. J. Physiol., 1931,*  
35 *96, 562–568; J. H. Barbee and G. R. Cokelet, Microvasc. Res., 1971, 3, 17–21*). For that  
36 reason, our study includes the effect of channel geometry by changing the hydraulic diameter  
37 of the channel as depicted in Fig. 5.(b) of the revised manuscript, by essentially tuning the  
38 smallest dimension of the channel cross section which we term as width.

39  
40  
41  
42  
43  
44  
45 **#2 Referee's comment:** *Shear thinning behavior is generally presented with variation of*  
46 *viscosity with shear rate, not shear stress. Please modify the related graphs (e.g. Fig. 2). I am*  
47 *also surprised to see that upon glutaraldehyde-fixation, RBCs continued to show the shear*  
48 *thinning behavior (Supplementary Figure). This is in contradiction to previous reports*  
49 *(Castellini et al., 2010, Front. Physiol.) and hence, must be clarified. Authors should indicate*  
50 *in Figs. 2 and 4 where they are using s.d. or s.e.m. as error bars.*

51  
52 **#2 Authors' response:** In accordance to the reviewer's suggestions, we have modified the  
53 figures (Fig 3 in the revised manuscript and Figure S2, in supplementary information).

54  
55 In accordance to the previous report *Castellini et al., 2010, Front. Physiol., ‘rigid RBC are*  
56 *unable to deform in response to shear forces and have a higher viscosity compared to normal*  
57

cells at shear rates above about  $10 \text{ s}^{-1}$ . From our experimental investigation, we found similar behaviour i.e. GA treated RBCs have more viscosity as compared to normal RBCs for a particular value of shear rate (as seen in Figure S2 in supplementary document). This issue has been delineated in the revised version of our manuscript.

We have used standard deviations (s.d.) of the results obtained from the repeated sets of experiments as error bars. We have mentioned this specific point in the captions of the figures in the revised manuscript.

**#3 Referee's comment:** *I don't agree with the claim that in Figure 4b, experimental and simulation trends agree with each other. In this graph, especially at 200 and 300 rpm, they deviate from each other not only by large values but also by the qualitative nature of the trends. Experimental trends saturate at higher  $W$  values, while theoretical values continue to rise. How do the authors explain this deviation? Such explanation and then, possible modification of the model to match these trends might be necessary to provide effective operational guidelines.*

**#3 Authors' response:** Authors would like to thank the reviewer for highlighting the above point. Possibly, at higher speed of rotation, mechanical vibration of the experimental set-up plays a key role, which results in the observed deviation between experimental and simulation results.

During the flow of blood through micro-conduits, there is formation of cell free layer (CFL) zone in the close vicinity of the wall (*R. Fahraeus et al, Am. J. Physiol., 1931, 96, 562–568*). This phenomenon is reported to have prominent effect while downsizing the channel hydraulic diameters (*A R. Pries et al, Am. J. Physiol., 1992, 263, 1770–1778*). According to *A R. Pries et al.*, the magnitude of apparent viscosity of blood will saturate for higher values of the channel hydraulic diameter, which supports our experimental findings of Fig. 5b (where the Q value saturates for higher width of the channel).

Due to the differences between experimental and theoretical results at higher rotational speeds, the effective operational range of the device is recommended to be constrained within 200 rpm, considering a balance between the rapidity of the test and its predictive reliability in tune with the design simulations.

**#4 Referee's comment:** *Do the authors include hematocrit level in the simulation? It should be clearly pointed out. Also, why there is no theory-model correspondence in Fig. 3?*

**#4 Authors' response:** We have followed a modified Casson model to simulate the blood flow through micro-channel, which includes hematocrit level in the simulation. The constitutive behaviour, as a function of the hematocrit fraction, accordingly reads (*Y. C. Fung, Biomechanics. Mechanical properties of living tissues, Springer, Berlin, 1993*):

$\mu_{\text{eff}} = \sqrt{\mu_{\infty}} + \sqrt{\tau_y/\dot{\gamma}}$ ;  $\mu_{\infty} = \mu_0(1-H)^{-2.5}$ ,  $\tau_y = 0.01(0.625H)^3$ ;  $H$  denotes the hematocrit fraction, and  $\dot{\gamma}$  is the strain rate.

Since three-dimensional computational studies are time consuming, so we have performed numerical simulations with a step of 50 rpm. Within the constraints of such discretization paradigm, the numerical and experimental predictions on burst frequency may indeed be compared. In the revised version of the manuscript, the issue has been taken care of, by plotting the experimental and numerical data within the same graph (as shown in Fig. 4).

**Minor Points:**

**#1 Referee's comment:** *Please give schematic showing the set-up used in simulation.*

**#1 Authors' response:** The schematic of the simulation set-up has been incorporated in the revised version of the manuscript as 'Fig 2'.

**#2 Referee's comment:** *Burst frequency should be defined in the very beginning.*

**#2 Authors' response:** This particular issue has been addressed in the revised version of the manuscript, by defining the burst frequency as the threshold frequency below which the fluid column will not burst into the channel from the reservoir.

**#3 Referee's comment:** *Please break complex sentences to simple ones for better readability.*

**#3 Authors' response:** Authors would like to thank for such suggestions. This has been taken care of in the revised manuscript.

Cite this: DOI: 10.1039/c0xx00000x

www.rsc.org/xxxxxx

## COMMUNICATION

### Effect of Hematocrit on Blood Dynamics on a Compact Disc Platform

Shantimoy Kar<sup>1</sup>, Monika Dash<sup>2</sup>, Tapas Kumar Maiti<sup>1,3</sup> and Suman Chakraborty<sup>\*1,4</sup>

Received (in XXX, XXX) XthXXXXXXXXXX 20XX, Accepted Xth XXXXXXXXXXXX 20XX

DOI: 10.1039/b000000x

We investigate blood flow dynamics on a rotationally actuated lab-on-a-compact disk (LOCD) platform, as a function of the hematocrit level of the blood sample. In particular, we emphasize on the resultant implications on the critical fluidic parameters like burst frequency and volumetric flow rate. Our results can be utilized as a characteristic guideline to predict the hematological parameters of a given small amount of blood sample from the observed flow characteristics, and can give rise to a new paradigm of medical diagnostics driven by interactions between blood rheology and rotational forces on an inexpensive platform, with minimal sample consumption.

**Keywords:** Lab-on-a-compact-disk (LOCD), hematocrit, burst frequency, rotational actuation.

Patho-physiological conditions of human body can be greatly understood with experimentations on blood samples. Blood consists of two major components, namely the cellular component and the plasma. Rheology of blood is known to be a strong function of the hematocrit value (i.e. the volume fraction of red blood cells (RBCs) with respect to the whole blood volume) and mechanical properties of RBCs<sup>1</sup>. It is well-known that 45% of the blood volume is occupied by RBCs, which indicates that particular haematological disorders (such as those due to altered hematocrit (Hct) values) are likely to be influenced based on RBC-related parameters<sup>1-3</sup> and accordingly alter the bulk flow characteristics. It is a well-established fact that blood rheology is dependent on several parameters like size, morphology, mechanical properties of cells, plasma chemistry and cellular interactions (RBC aggregation)<sup>4-6</sup>. As the morphology of RBCs is altered in case of few diseases like malaria, anaemia, sickle cell diseases<sup>1-3</sup>, the blood rheology is also accordingly affected. Accordingly, rheological parameters can be used as monitoring tools for the diagnosis of such diseases. Researchers have previously explored 'cellular-scale-hydrodynamics'<sup>7</sup> to understand the rheological aspects of blood and have subsequently showed that several disorders can be identified based on the blood rheology<sup>8</sup>. However, a close review of the concerned literature suggests that the detection of haematological disorders using bulk fluid dynamic characteristics of blood on a simple rotational platform is yet to be explored in an exhaustive manner, unveiling an explicit interlinkage between rotational flow dynamics and blood rheology.

Recent advancements in miniaturized lab-on-a-chip based technologies (like paper-based<sup>9,10</sup> and thread-based diagnostics<sup>11</sup>) have given a huge boost to the healthcare industry. These lab-on-a-chip based technologies have gained prominence due to a number of inherent advantages they offer, like automation and

parallel handling of liquid samples, low volume of sample consumption, as well as providing rapid and portable diagnostic paradigms. Various processes like sample preconditioning, sequential valving, incubation, mixing and washing have previously been investigated on such miniaturized platforms<sup>12,13</sup>. Usage of such lab-on-a-chip devices (especially glass, silicon, and PDMS based etc.)<sup>14,15</sup> are severely restricted by the associated fabrication protocols, which take the perspective applications of these devices far away from an inexpensive paradigm. Thus, the choice of point-of-care diagnostic platform is often dictated through a compromise between the analytical efficiency and frugality of the device. Towards removing these deficiencies, out of several existing platforms, lab-on-a-compact disk (LOCD) is one of the best choices due to its cost-effective manufacturing process, multiplexing (a large number of tests can be done on a single compact disc, simultaneously) and efficient integrability of standard analytical protocols<sup>12,13,16</sup>. Flow in such devices is actuated by rotational forces, which eliminates the need of external pumping mechanisms to actuate the flow within the micro-conduits.

In an effort to detect the haematological disorders, a number of methodologies have been employed by the previous researchers, which includes visualization of the morphological alterations at cellular level, or more specifically at the single-cell level<sup>17</sup>. Although the importance of experimentations at cellular scales cannot be under-emphasized, these experimentations are bounded by several limitations like the requirement of sophisticated instruments and trained personnel. These short-comings urge the need of other inexpensive methodologies. In an effort to address these shortcomings, here we employ a microfluidics based lab-on-a-compact disk (LOCD) platform (Fig. 1a) to investigate the dynamics of blood, containing varying levels of hematocrit (Hct). We characterize the dynamics of blood with two basic parameters

of LOCD platform, namely the burst frequency ( $f_b$ ) (i.e. the threshold frequency below which the fluid column will not burst into the channel from the reservoir) and the volumetric flow rate ( $Q$ ). In addition to the experimental investigation, we perform numerical simulations of blood flow through micro-confinements subject to rotational forces, where we use modified Casson model to describe the blood rheology. The choice of modified Casson model is made based on the fact that it is one of the very few available models<sup>18–20</sup> which incorporates the effects of hematocrit (Hct) levels in the constitutive behaviour of blood<sup>5,6</sup>. Since our aim is to quantify the Hct levels based on the flow characteristics, the choice of Casson model is well suited for the present purpose. We subsequently show that reasonably good agreement is observed between the experimental findings and the numerical simulations, thereby offering a simple design basis for blood diagnostics driven by interactions between fluid rheology and rotational actuation.

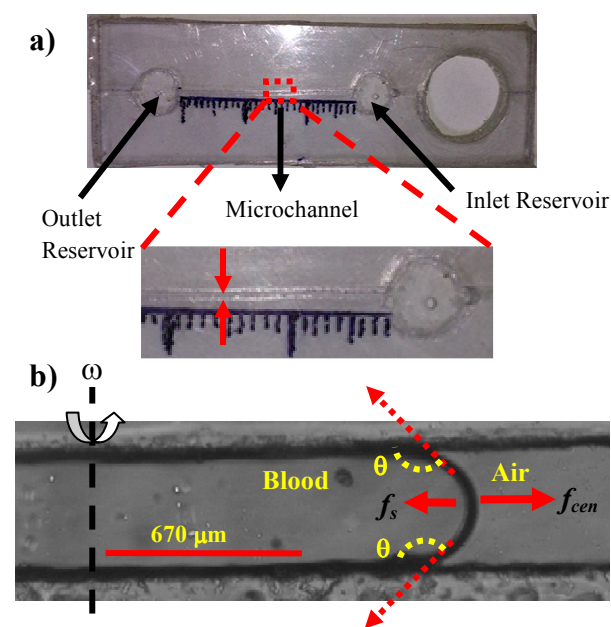


**Fig 1:** **a)** Image of the device contains a single channel (straight channel connected with two reservoirs, used for the experiment). The blown up image shows the microchannel within the device and **b)** depicts the microscopic view (captured through an inverted microscope (OLYMPUS IX71), with 10X objective lens) of the moving liquid front traversing through the microchannel.

## Materials and Methods

We fabricate the LOCD devices through stacking method<sup>21</sup>. We stacked 5 different layers, out of which, three are made of polymethyl-methacrylate (PMMA) (Lexan, GE) and the rest of the two are made of pressure-sensitive-adhesives (PSA) (FLEX mount DFM 200 clear V-95, 3M, Flexcon, Inc., Spencer, MA). PSA sheets are used in between two PMMA layers to attach the adjacent layers<sup>13</sup>. The channels are fabricated by cutting the adhesive layers. While executing the experiments, we rotate the LOCD platform by integrating the system with a servo-motor (SureServo<sup>TM</sup> AC Servo Systems), which provides judicious

tuning of flow actuation rates. We use a straight channel having a length of 2.9 cm connected with two circular reservoirs of 0.6 cm diameter and a height of 100  $\mu\text{m}$ , for typical blood flow diagnostics.

As the Hct value of healthy human body varies from 35% to 55%, we use blood samples with a range of hematocrit levels, ranging from 37% to 53% in our experiments; which closely resemble physiological conditions in human bodies. The blood samples, mixed with an anti-coagulant, were stored at 4°C. We have executed the experiments for four different channel widths (essentially, the smallest dimension of the channel cross section that dictates the hydraulic diameter): 200  $\mu\text{m}$ , 350  $\mu\text{m}$ , 500  $\mu\text{m}$ , and 700  $\mu\text{m}$ . All the experiments were conducted by following the institutional ethical guidelines.

## Theoretical Modelling

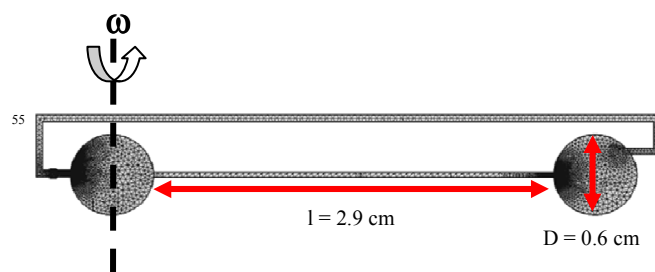


**Fig 2:** Schematic representation of the set-up used for numerical simulation. The dimensions of the channels employed for the simulation are: length ( $l$ ) = 2.9 cm, height ( $h$ ) = 100  $\mu\text{m}$ , and four different widths ( $w$ ) = 200  $\mu\text{m}$ , 350  $\mu\text{m}$ , 500  $\mu\text{m}$ , and 700  $\mu\text{m}$ ; the diameter of the inlet and outlet reservoir are 0.6 cm. Both the source and sink reservoirs are connected through a venting channel to allow the removal of air from the outlet reservoir and the channel, while the advancing meniscus of blood moves towards the outlet reservoir.

To study the filling dynamics of blood inside the rotating platform (as shown in Fig 2), the level set method<sup>22,23</sup> was used coupled with the continuity and the momentum conservation equations. Three dimensional simulations were performed using commercially available finite element based package COMSOL Multiphysics 4.3a. Under the paradigm of level set method, a level set function  $\phi$  is defined over the whole domain. This method removes the complications associated with explicit interface tracking, since the two separate phases (air and blood) are defined by two distinct values of  $\phi$ : we define  $\phi = 0$  for air and  $\phi = 1$  in blood. Consequently, the interface is defined by  $\phi = 0.5$ . The level set function is governed by the following equation<sup>23,24</sup>

$$\frac{\partial \phi}{\partial t} + \vec{u} \cdot \nabla \phi = \gamma \nabla^2 \left[ \varepsilon \nabla \phi - \phi(1-\phi) \frac{\nabla \phi}{|\nabla \phi|} \right]$$

where  $\varepsilon$  determines the thickness of the interface and  $\gamma$  dictates the amount of re-initialization. The governing differential equations for fluid flow are as follows:



$$\nabla \cdot \bar{\mathbf{u}} = 0$$

$$\rho \left( \frac{\partial \bar{\mathbf{u}}}{\partial t} + \bar{\mathbf{u}} \cdot \nabla \bar{\mathbf{u}} \right) = -\nabla p + \nabla \cdot \left[ \mu_{eff} (\nabla \bar{\mathbf{u}} + \nabla \bar{\mathbf{u}}^T) \right] + \vec{f}_s + \vec{f}_r$$

According to the modified Casson model, the effective viscosity<sup>19</sup>

$$\mu_{eff} = \sqrt{\mu_\infty} + \sqrt{\tau_y / \dot{\gamma}}; \quad \mu_\infty = \mu_0 (1-H)^{-2.5},$$

$$\tau_y = 0.01(0.625H)^3 \text{ and } H \text{ denotes the hematocrit fraction and } \dot{\gamma}$$

is the strain rate. Further, on a rotating platform, the momentum equation contains additional body force terms  $\vec{f}_s$  and  $\vec{f}_r$ , where

$\vec{f}_s$  denotes the body force generated due to the surface tension and  $\vec{f}_r$  is the body force due to rotational actuation. These body forces can be mathematically expressed

$$\text{as: } \vec{f}_r = -\rho \left[ \underbrace{\bar{\omega} \times (\bar{\omega} \times \vec{r})}_{\text{centrifugal}} + \underbrace{2\bar{\omega} \times \vec{V}_{xyz}}_{\text{Coriolis}} + \underbrace{(\bar{\omega} \times \vec{r})}_{\text{Euler}} \right];$$

$$\vec{f}_r = \vec{f}_{\text{centrifugal}} + \vec{f}_{\text{Coriolis}} + \vec{f}_{\text{Euler}}$$

$$\vec{f}_s = \nabla \cdot \mathbf{T} \text{ where } \mathbf{T} = \sigma (\mathbf{I} - (\mathbf{nn}^T)) \delta$$

Here  $\rho$  is the blood density,  $p$  is the pressure,  $\bar{\mathbf{u}}$  is the blood flow velocity,  $\bar{\omega}$  is the angular velocity of the CD,  $\bar{\omega}$  is its angular acceleration,  $\vec{V}_{xyz}$  is the velocity of the blood relative to the rotating reference frame xyz attached to the CD, and  $\vec{r}$  is the position vector. Further  $\sigma$  denotes the surface tension coefficient,  $\mathbf{n}$  is the interface normal,  $\mathbf{I}$  is the identity matrix and  $\delta$  is the Dirac delta function which is nonzero only at the fluid interface.

In the present case, this function is defined as<sup>22</sup>:

$$\delta = 6|\phi(1-\phi)| |\nabla \phi|$$

Initially, the source reservoir and half of the channel are considered to be filled with blood and rest with air. Simulations with blood only in the source reservoir to start with, did not give very different results from this design but just added on the computational time. The rotational speed is increased in steps of 50 rpm to determine the burst frequency. If it bursts at certain point, lower frequencies are considered. The study type is chosen as transient with phase initializations. We have used the following boundary conditions: i) wetted wall boundary condition and no penetration at the walls, ii) inlet and outlet pressures were set at atmospheric pressure i.e., 103125 Pa. (gauge pressure = 0). The incorporation of wetted wall boundary conditions is necessary to capture the essential physics of blood dynamics<sup>20,25</sup>. The wetted wall boundary condition makes it feasible to set a specific value of contact angle [Table 1 of ESI].

## Results and Discussions

As mentioned earlier, the flow characteristics of blood are greatly dependent on the blood rheology, which, in turn, is significantly affected by the Hct and channel diameter<sup>26</sup>. Being a heterogeneous fluid, blood shows shear thinning behaviour (Fig. 2). At higher shear rate, however, blood has been demonstrated to

behave like a Newtonian fluid<sup>27,28</sup>. For a particular shear rate, for higher values of Hct, the magnitude of effective viscosity will also be higher (as observed in Fig. 3) because of higher amount of aggregation between red blood cells. On the other hand, for lower Hct, this phenomenon is less pronounced which reduces the effective viscosity. Increase in viscosity at low actuation rates is a direct manifestation of cell-sedimentation, which is subsequently followed by aggregation of RBCs<sup>29</sup>.

The valving of fluid from the inlet reservoir is governed by the balance of centrifugal forces and the capillary forces<sup>30</sup>. It has been previously reported that, the fluid column will burst into the channel from the reservoir when the frequency of rotation exceeds a threshold value, which is termed as burst frequency<sup>31,32</sup>. Below the threshold frequency, the fluid will not come out from the inlet reservoir, as the capillary force overshadows the centrifugal force (these forces tend to oppose each other, for the contact angles addressed here). Beyond the threshold frequency, however, the centrifugal force overcomes the surface tension force, and the fluid starts flowing in the radial direction (as shown in Fig. 1b).

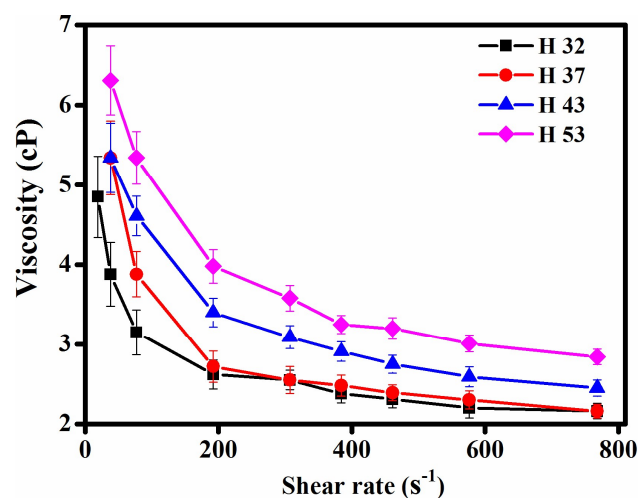


**Fig 3:** Viscosity vs. shear rate characteristics for different hematocrit levels of blood measured through a viscometer (Brookfield Viscometer DV-II+ Pro). The graph depicts the shear thinning behaviour of blood. It is also seen that for a particular shear rate, the viscosity is higher for higher value of hematocrit. The error bars indicates standard deviation (s.d.) of the results from repeated set of experiments.

Since, Hct dictates the volume of RBC with respect to the total volume of blood, any alterations in Hct is expected to be reflected in the flow characteristics of blood. From Fig. 4, it is seen that for a particular channel width, the value of burst frequency ( $f_b$ ) increases with the increase of Hct from 37 to 53. Experimental observations show that this increase is in the range of 24-28.4%, for the corresponding Hct levels. This particular observation can be delineated from the fact that for higher value of Hct, the rate of aggregate formation of RBCs is high, which eventually enhances the effective viscosity of blood. Therefore, higher centrifugal forces, and hence higher rotational frequencies, are required for bursting of fluid column into the sink reservoir.

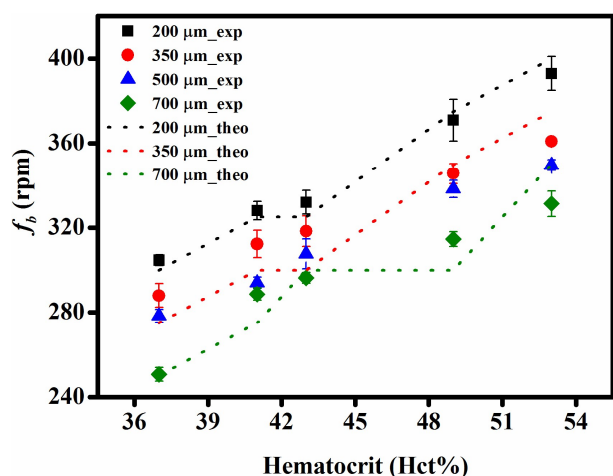


Fig 4. Effect of hematocrit on burst frequency; the theoretical and experimental findings are merged in the same figure. Scattered data points represent the experimental findings whereas the dotted lines represent the theoretical results. The error bars indicates standard deviation (s.d.) of the results from repeated set of experiments.

Fig. 5.(a) delineates the volumetric flow rate as a function of the rpm, for varying hematocrit levels, for a fixed channel width (350  $\mu\text{m}$ ). From this figure, it seems that the volumetric flow rate ( $Q$ ) decreases with the increase of Hct for a particular channel width. This decrease in the volumetric flow rate can be explained from the fact that for lower Hct levels; the effective viscosity of blood is low, which finally results in higher flow rates. This observation is consistent with the previous figure, where it was shown that higher values of Hct lead to higher bursting frequencies.

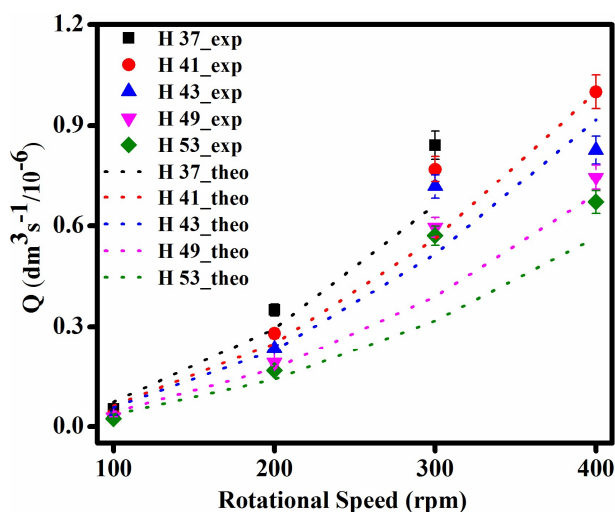


Fig 5a. Volumetric flow rate characteristics as a function of rotational speed (rpm) for different Hct% (for a specific channel width of 350  $\mu\text{m}$ ); the theoretical and experimental findings are merged in the same figure. Scattered data points represent the experimental findings whereas the dotted lines are theoretical findings. The error bars indicates standard deviation (s.d.) of the results from repeated set of experiments. In the figure caption, the abbreviation theo means theoretical and the abbreviation exp means experimental data.

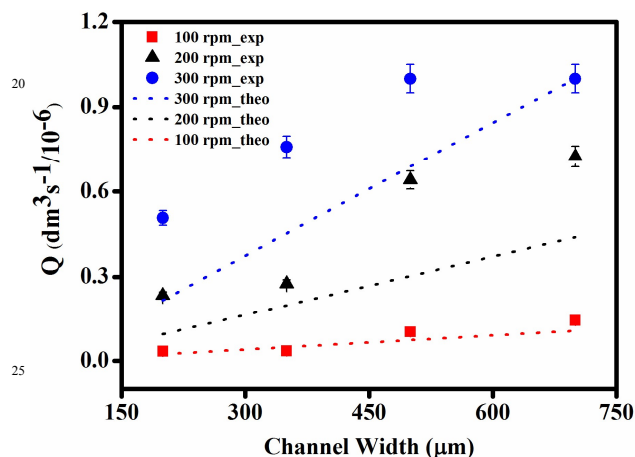


Fig 5b. Volumetric flow rate characteristics as a function of channel width ( $\mu\text{m}$ ) for a sample having Hct% value of 37; the theoretical and experimental findings are merged in the same figure. Scattered data points represent the experimental findings whereas the dotted lines represent the theoretical results. The error bars indicates standard deviation (s.d.) of the results from repeated set of experiments.

It is also important to note in this context that blood dynamics is significantly altered with variations in the hydraulic diameter of the conduit through which it is being transported. During the blood flow through microchannel, RBCs do not distribute themselves evenly across the cross-section of the channel. The concentration of RBCs is more at the central zone of the channel as compared to the vicinity of the channel-wall<sup>33</sup>. This heterogeneity of cell distribution is the manifestation of the net hydrodynamic force. For a particular Hct, higher the channel hydraulic diameter, lower is the extent of cell free layer (CFL). Hence the effective viscosity becomes lower for higher hydraulic diameter, which makes the volumetric flow rate higher. The heterogeneous distribution of cells is known to be altered with the channel hydraulic diameter<sup>26,32-34</sup>. For that reason, our study includes the effect of channel geometry by changing the width of the channel as depicted in Fig. 5.(b). It can be observed from this figure that with increasing channel width,  $Q$  increases for a specific value of Hct. The rate of flow enhancement is more pronounced at lower channel widths (200  $\mu\text{m}$  to 350  $\mu\text{m}$ ), whereas, the rate of flow enhancement gradually decreases as we move towards higher channel widths (350  $\mu\text{m}$  to 700  $\mu\text{m}$ ). In addition to the experimental results, we also plot our numerical results in figure 5.(b). While good agreements between experimental and theoretical predictions are found for lower rotational speeds, the discrepancies between them at higher rotational speeds may be attributed to uncertainties in experimental observations at augmented levels of setup vibration.

In case of few diseases like malaria, sickle cell anaemia, the malleability of RBC surface is significantly enhanced as compared to the normal healthy RBCs, and consequently the rheology of blood is changed. Researchers have attempted to mimic such rheological alteration by treating normal RBCs with glutaraldehyde (GA)<sup>35</sup>. Due to the chemical functionality of GA,

the RBC surface is known to be cross-linked and consequently the morphology of RBC (Figure S1 of ESI) is altered. To validate our hypothesis of diagnosing the disease by exploiting blood rheology, we have performed viscosity ( $\eta$ ) measurements as a function of shear rate for GA-treated blood samples. Significant difference (~66%) is observed between the normal RBCs and GA-treated RBCs<sup>4</sup> (Figure S2 in ESI) in terms of viscosity values, thus supporting our approach of diagnostics.

## Conclusions

In summary, we report a flow characterization of human blood samples on a centrifugally actuated LOCD platform, parametrized as a function of the hematocrit level. Our investigation unveils the dependence of channel geometry and Hct on blood flow dynamics on a compact disc. We have characterized the dynamic flow features in terms of two pertinent parameters, namely burst frequency and volumetric flow rate. Our experimental findings closely follow the similar trends as obtained from theoretical findings following a modified Casson model, although the absolute value of the parameters differs in magnitude to an extent that depends on the rotational speed of the diagnostic platform. This difference between the theoretical and experimental results can be ascribed to the increasing uncertainties in the flow diagnostics at higher rotational speeds, on account of mechanical vibrations of the experimental set-up. Accordingly, due to the differences between experimental and theoretical results at higher rotational speed, the effective operational range of the device is recommended to be constrained within 200 rpm, considering a balance between the rapidity of the test and its predictive reliability in tune with the design simulations.

Practical consequences of our investigations, in the field of pathological diagnostics, can be immense. We envision that this specific study can act as a potential guideline to find out a well-calibrated fluid dynamics based diagnostic parameter for capturing haematological disorders, without necessitating chemical test. Following that paradigm, this particular approach can be utilized to predict the Hct value of the blood sample from the burst frequency value through a cross-correlation and therefore can be used as a deterministic tool for finding out the relevant pathological conditions, thereby unveiling a new paradigm of highly inexpensive chemical free pathological diagnostics on a simple rotational platform.

## Notes and references

<sup>1</sup>Advanced Technology Development Centre, Indian Institute of Technology Kharagpur, Kharagpur-721302; <sup>2</sup>Department of Physics, Indian Institute of Science Education and Research Pune, Pune-411008; <sup>3</sup>Department of Biotechnology, Indian Institute of Technology Kharagpur, Kharagpur-721302; <sup>4</sup>Department of Mechanical Engineering, Indian Institute of Technology Kharagpur, Kharagpur-721302, India.

Email: [suman@mech.iitkgp.ernet.in](mailto:suman@mech.iitkgp.ernet.in)

† Electronic Supplementary Information (ESI) available: See DOI: 10.1039/b000000x/

**Acknowledgement:** SK would like to thank Council of Scientific and Industrial Research (CSIR), India for his research fellowship. Authors would like to express their sincere thanks to Mr. Ranabir Dey for his assistance at the initial stage of the work. They would also like to thank the financial support provided by SRIC IIT Kharagpur under the

60 Sponsored Project titled “Center of Excellence for Training and Research in Microfluidics”.

- O. K. Baskurt and H. J. Meiselman, *Semin. Thromb. Hemost.*, 2003, **29**, 435–450.
- F. K. Glenister, R. L. Coppel, A. F. Cowman, N. Mohandas, and B. M. Cooke, *Blood*, 2002, **99**, 1060–1063.
- M. Diez-Silva, M. Dao, J. Han, C.-T. Lim, and S. Suresh, *MRS Bull.*, **35**, 382–388.
- M. a Castellini, O. Baskurt, J. M. Castellini, and H. J. Meiselman, *Front. Physiol.*, 2010, **1**, 146.
- J. D. Enderle, S. M. Blanchard, and J. D. Bronzino, *Introduction to Biomedical Engineering*, Academic Press, San Diego, Third., 2005.
- D. J. Schneck and C. L. Lucas, *Biofluid Mechanics*, University Press, New York, New York, 1990.
- M. Abkarian, M. Faivre, R. Horton, K. Smistrup, C. a Best-Popescu, and H. a Stone, *Biomed. Mater.*, 2008, **3**, 034011.
- L. Dintenfass, *Angiology*, 1974, **25**, 365–372.
- A. W. Martinez, S. T. Phillips, G. M. Whitesides, and E. Carrilho, *Anal. Chem.*, 2010, **82**, 3–10.
- A. K. Yetisen, M. S. Akram, and C. R. Lowe, *Lab Chip*, 2013, **13**, 2210–51.
- X. Li, J. Tian, and W. Shen, *ACS Appl. Mater. Interfaces*, 2010, **2**, 1–6.
- J. Ducerée, S. Haeberle, S. Lutz, S. Pausch, F. Von Stetten, and R. Zengerle, *J. Micromechanics Microengineering*, 2007, **17**, S103–S115.
- M. Madou, J. Zoval, G. Jia, H. Kido, J. Kim, and N. Kim, *Annu. Rev. Biomed. Eng.*, 2006, **8**, 601–28.
- H. Becker and L. E. Locascio, *Talanta*, 2002, **56**, 267–287.
- S. K. Sia and G. M. Whitesides, *Electrophoresis*, 2003, **24**, 3563–3576.
- R. Gorkin, J. Park, J. Siegrist, M. Amasia, B. S. Lee, J.-M. Park, J. Kim, H. Kim, M. Madou, and Y.-K. Cho, *Lab Chip*, 2010, **10**, 1758–73.
- M. Abkarian, M. Faivre, and H. a Stone, *Proc. Natl. Acad. Sci. U. S. A.*, 2006, **103**, 538–42.
- B. M. Johnston, P. R. Johnston, S. Corney, and D. Kilpatrick, *J. Biomech.*, 2004, **37**, 709–20.
- Y. C. Fung, *Biomechanics. Mechanical properties of living tissues*, Springer, Berlin, 1993.
- S. Chakraborty, *Lab Chip*, 2005, **5**, 421–430.
- D. Chakraborty, R. Gorkin, M. Madou, L. Kulinsky, and S. Chakraborty, *J. Appl. Phys.*, 2009, **105**, 084904.
- 2012, 1–16.
- Y. Lin, *Electrophoresis*, 2013, **34**, 736–44.
- E. Olsson, G. Kreiss, and S. Zahedi, *J. Comput. Phys.*, 2007, **225**, 785–807.
- S. Chakraborty, *Anal. Chim. Acta*, 2007, **605**, 175–84.
- A. R. Pries, D. Neuhaus, and P. Gaetgens, *Am. J. Physiol.*, 1992, **263**, 1770–1778.
- D. A. Fedosov, W. Pan, B. Caswell, G. Gompper, and G. E. Karniadakis, *Proc. Natl. Acad. Sci. U. S. A.*, 2011, **108**, 11772–11777.
- R. L. Fournier, *Basic Transport Phenomena in Biomedical Engineering*, CRC Press, The University of Toledo Ohio, USA, 3rd edn.
- J. J. Bishop, a S. Popel, M. Intaglietta, and P. C. Johnson, *Biorheology*, 2001, **38**, 263–274.
- H. Cho, H. Y. Kim, J. Y. Kang, and T. S. Kim, *J. Colloid Interface Sci.*, 2007, **306**, 379–385.
- T. H. G. Thio, S. Soroori, F. Ibrahim, W. Al-Faqheri, N. Soin, L. Kulinsky, and M. Madou, *Med. Biol. Eng. Comput.*, 2013, **51**, 525–535.
- A. Kazemzadeh, P. Ganesan, F. Ibrahim, S. He, and M. J. Madou, *PLoS One*, 2013, **8**, e73002.
- R. Fahraeus and T. Lindqvist, *Am. J. Physiol.*, 1931, **96**, 562–568.
- J. H. Barbee and G. R. Cokelet, *Microvasc. Res.*, 1971, **3**, 17–21.
- A. M. Forsyth, J. Wan, W. D. Ristenpart, and H. A. Stone, *Microvasc. Res.*, 2007, **80**, 37–43.

1  
2  
3  
4  
5  
6  
7  
8  
9  
10  
11  
12  
13  
14  
15  
16  
17  
18  
19  
20  
21  
22  
23  
24  
25  
26  
27  
28  
29  
30  
31  
32  
33  
34  
35  
36  
37  
38  
39  
40  
41  
42  
43  
44  
45  
46  
47  
48  
49  
50  
51  
52  
53  
54  
55  
56  
57  
58  
59  
60

Analyst Accepted Manuscript

## Electronic Supplementary Information

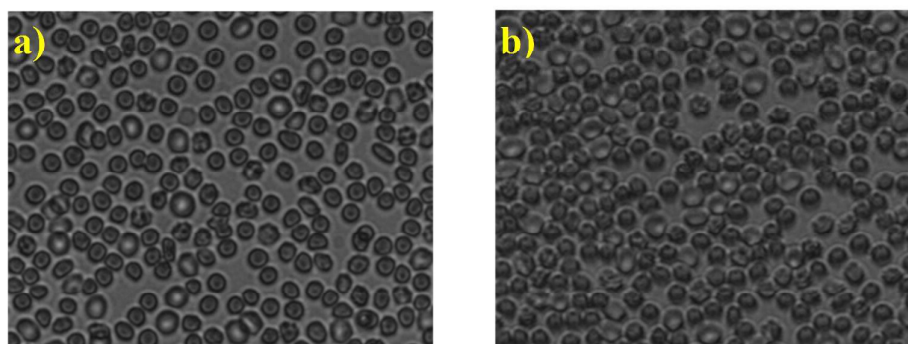


**Figure S1:** The above figure depicts the microscopic images of a) normal RBCs and b) glutaraldehyde (GA) treated RBCs. Sample specification: a) (10  $\mu\text{l}$  blood+ 990  $\mu\text{l}$  phosphate buffer saline (PBS) and b) (10  $\mu\text{l}$  blood+980  $\mu\text{l}$  PBS+10  $\mu\text{l}$  GA. There is an alteration in RBC morphology after GA treatment (as the regular shape of RBC is changed). The images were captured through an inverted microscope (OLYMPUS IX71), with 40X objective lens. This particular morphological alteration leads to the rheological alteration (as discussed in Figure S2).

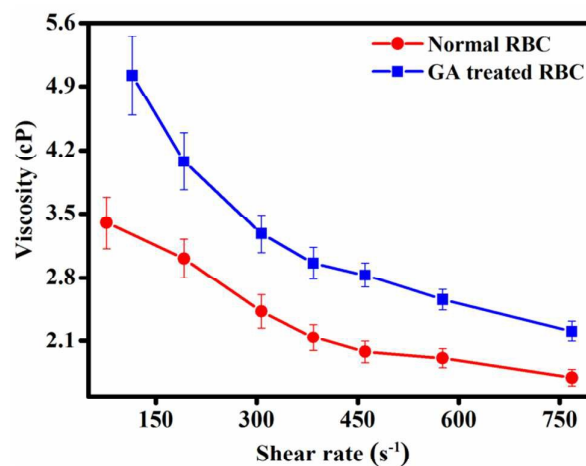


**Figure S2.** Viscosity vs. shear rate characteristics between normal RBC and glutaraldehyde (GA) treated RBC. Viscosity measurement was done through a viscometer (Brookfield Viscometer DV-II+ Pro). Sample specification (10  $\mu\text{l}$  blood+ 990  $\mu\text{l}$  phosphate buffer saline (PBS) and (10  $\mu\text{l}$  blood+980  $\mu\text{l}$  PBS+10  $\mu\text{l}$  GA).

**Table 1:**

Hct%	Contact angle (in degrees)	Surface tension coefficient (N/m)
37	64.95	0.05079
41	65.85	0.0521
43	66.42	0.05416
49	70.79	0.05538
53	71.15	0.06589

We have measured the contact angle of blood for different hematocrit values, on PMMA surface using a Rame-Hart (model 500) goniometer and have subsequently determined the value of surface tension coefficient using ImageJ software. Afterwards, the calculated values of surface tension coefficient have been fed in during simulations. The experimental values of contact angles and surface tension coefficients are tabulated in Table 1.